— Supporting Information —

Exchange Bias in Magnetic Topological Insulator Superlattices

Jieyi Liu,[*,†,¶] Angadjit Singh,[‡,§] Yu Yang Fredrik Liu,[‡] Adrian Ionescu,[‡] Balati Kuerbanjiang,[†] Crispin H. W. Barnes,[‡] and T. Hesjedal[*,†]

†*Clarendon Laboratory, Department of Physics, University of Oxford, Parks Road, Oxford, OX1 3PU, United Kingdom*

‡*Cavendish Laboratory, University of Cambridge, J. J. Thomson Avenue, Cambridge, CB3 0HE, United Kingdom*

¶*Cavendish Laboratory, University of Cambridge, J. J. Thomson Avenue, Cambridge, CB3 0HE, United Kingdom*

§*Department of Physics, Royal Holloway, University of London, Egham Hill, Egham, TW20 0EX, United Kingdom*

E-mail: Jieyi.Liu@physics.ox.ac.uk; Thorsten.Hesjedal@physics.ox.ac.uk

S1. Methods

Sample growth

The $[CST/DBT]_{10}$ superlattices were grown on *c*-plane sapphire substrates using molecular beam epitaxy (MBE), with a base pressure of 1×10^{-10} mbar. Prior to the thin film growth, the substrates were cleaned in solvents and rinsed in DI water, degassed overnight in the preparation chamber, and heat-treated at 450 °C for up to 30 minutes in the growth chamber. Bi, Sb and Te (99.9999% purity) were evaporated from standard effusion cells, while Cr and Dy (99.99% purity) were evaporated from high temperature effusion cells. A beam flux ratio of ∼1:10:100 for (Cr+Dy):(Bi+Sb):Te was maintained throughout the growth. The Te overpressure helps to reduce Te vacancies and anti-site defects common for the $(Bi,Sb)_2Te_3$ system.[1] As a seed layer, a 3-nm-thick Bi_2Te_3 film was deposited onto the substrate at 250 °C, followed by an anneal at 300 °C under Te flux. The CST/DBT superlattice consists of 10 repeats of nominally 5-nm-thick DBT layers and 10-nm-thick CST layers, grown at 300 °C. Based on previous calibrations using a combination of Rutherford backscattering spectroscopy (RBS) and particle induced x-ray emission (PIXE), the nominal composition of the superlattice is $[Cr_{0.41}Sb_{1.59}Te_3/Dy_{0.62}Bi_{1.38}Te_3]_{10}$. Finally, an amorphous Bi layer was deposited as a capping layer to protect the sample from oxidation. The overall thickness of the superlattice (excluding the seed layer and the capping layer) is ∼150 nm. Following this general recipe, we also grew 20-nm-thick CST and DBT films on *c*-plane sapphire substrates as references, with nominal doping concentrations identical to the ones of the respective layers of the TI superlattice sample.

Device fabrication and transport measurements

The TI thin films were patterned into Hall bars measuring 1000 μm ×100 μm using standard optical lithography and Ar^+ ion milling, followed by the fabrication of Ohmic Ti/Au contacts (20 and 80-nm-thick) by thermal evaporation and lift-off. The devices were then mounted

onto 20-pin leadless chip carriers and the contacts were made by wire bonding. The chip carriers fit into the sample holder of a transport measurement probe, which was loaded into a ^{4}He continuous-flow cryostat. The electrical transport properties of the devices were measured using a standard four-terminal AC lock-in scheme with an input current of 1 μA at a frequency of 77 Hz.

MOKE measurements

Polar MOKE measurements were carried out in the same ^{4}He cryostat using a stand-alone MOKE probe which has been described in detail in Ref.[2] A continuous-wave laser beam with a wavelength of 850 nm was generated from a stabilized diode laser, and the light was polarized using a Glan-Taylor polarizer. The laser beam was then focused onto the TI film down to a 2.2 μm diameter spot size. The Kerr rotation of the reflected beam was modulated at 100 kHz by a photoelastic modulator before going through a second polarizer, and finally reaching the photodetector. The Kerr angle is proportional to the ratio between the AC (at 100 kHz) and DC photovoltages generated at the detector.

First-principles calculations

The DFT calculations were performed using the Vienna ab initio Simulation Package (VASP). The Perdew-Burke-Ernzerhof generalized gradient approximation (PBE-GGA) was applied for the exchange correlation functional. The projector augmented wave (PAW) method was employed, together with the plane wave basis set which had a kinetic energy cut-off of 520 eV. The structure relaxation was performed under the conjugated gradient optimization method, using the following convergence criteria: the residual forces must be less than 5×10^{-4} eV/Å, and the total energy must have converged to within 1×10^{-5} eV. A dense k-point grid was applied to compute the Brillouin-zone integrals, e.g., a Γ-centered $6 \times 6 \times 1$ grid was used for the calculations of an 30-atom cell.

Supplemental Figures

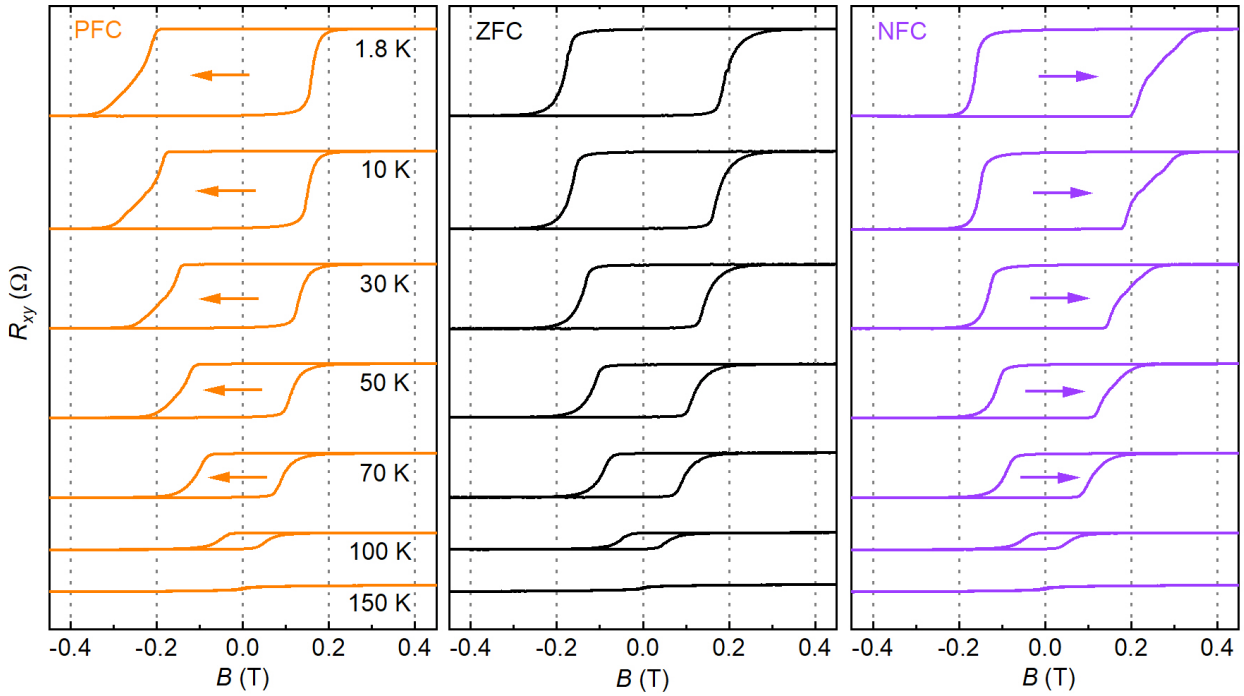

Figure S1: Exchange-biased hysteresis loops of the TI superlattice at different temperatures probed by electrical transport measurements. Positive-field-cooling (PFC) at +6 T results in a shift of the unbiased loop to the left (orange), and negative-field-cooling (NFC) at -6 T results in a shift to the right (purple). The unbiased loop (black), resulting from zero-field-cooling (ZFC), is shown as a reference.

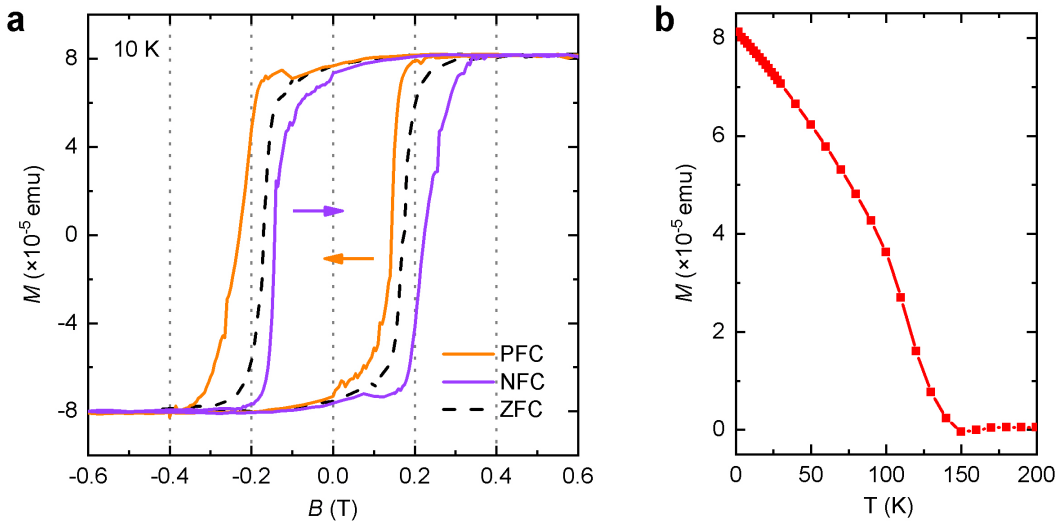

Figure S2: Exchange-biased magnetic response of the TI superlattice probed by SQUID magnetometry. (a) Hysteresis loops of the superlattice at 10 K. The measurements were conducted after positive-field-cooling (PFC) at +6 T (orange), after negative-field-cooling (NFC) at -6 T (purple), and after zero-field-cooling (ZFC) (black) from room temperature. (b) Temperature-dependent magnetization of the superlattice (ZFC case), measured at remanence.

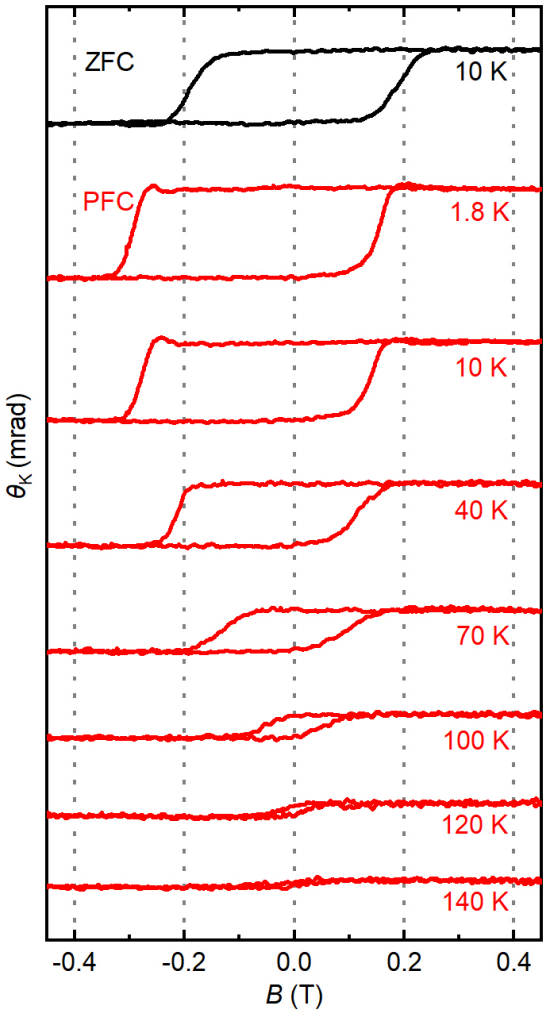

Figure S3: Exchange-biased hysteresis loops of the TI superlattice at different temperatures probed by MOKE measurements. Positive-field-cooling (PFC) at +6 T results in a shift of the unbiased loop to the left (red loops). The exchange bias effect is observed below 100 K, and hysteresis loops are present below 140 K. The zero-field-cooled (ZFC) hysteresis loop at 10 K is shown as a reference (black loop on top).

References

(1) Das, D.; Malik, K.; Deb, A. K.; Dhara, S.; Bandyopadhyay, S.; Banerjee, A. Defect induced structural and thermoelectric properties of Sb_2Te_3 alloy. *J. Appl. Phys.* **2015**, *118*, 045102.

(2) Liu, J.; Singh, A.; Llandro, J.; Duffy, L. B.; Stanton, M. R.; Holmes, S. N.; Applegate, M. J.; Phillips, R. T.; Hesjedal, T.; Barnes, C. H. W. A low-temperature Kerr effect microscope for the simultaneous magneto-optic and magneto-transport study of magnetic topological insulators. *Meas. Sci. Technol.* **2019**, *30*, 125201.